Measurements of CO_2 and energy fluxes over a mixed hardwood forest in the mid-western United States

Hans Peter Schmid*, C. Susan B. Grimmond, Ford Cropley, Brian Offerle, Hong-Bing Su

Department of Geography, Indiana University, Bloomington, IN 47405, USA

Abstract

Results from the first full year of measurements (1998–1999) of above canopy CO_2 and energy fluxes at the AmeriFlux site in the Morgan-Monroe State Forest, IN, USA, are presented. The site is located in an extensive secondary successional broadleaf forest in the maple-beech to oak-hickory transition zone. The minimum fetch is 4 km. Turbulent flux measurements are obtained by an eddy-covariance system at 46 m (1.8 times the canopy height) with a closed-path infrared gas analyzer.

Peak vegetation area index (VAI) was determined as 4.7±0.5 and the mean albedo during the vegetative period was 0.15±0.02. The aerodynamic roughness length was estimated as 2.1±1.1 m. It showed little variation with wind direction or season. The seasonal variations of energy partitioning and of net CO_2 exchange are discussed in terms of the phenological development of the forest. To estimate the annual net ecosystem production (NEP) and carbon sequestration, eddy-covariance measurements during periods of poorly developed turbulence at night, and missing data were replaced by a simple parametric model based on measurements of soil temperature and photosynthetically active radiation (PAR). The night-time flux correction reduces the annual sequestration estimate by almost 50%. The corrected estimate of annual NEP for the 1998–1999 season is 2.4 t C ha^{-1} per year ±10%. © 2000 Elsevier Science B.V. All rights reserved.

Keywords: AmeriFlux; Forest-atmosphere exchange; Eddy-covariance; Carbon sequestration; Forest micrometeorology

1. Introduction and background

This paper presents the first set of results (March 1998–February 1999, inclusive) from a long-term project measuring forest-atmosphere exchanges of CO_2, water vapor and energy balance components over the Morgan-Monroe State Forest (MMSF), a mixed deciduous forest in south-central Indiana in the mid-western United States.

The central objective of this research is to enhance empirical and theoretical understanding of soil-vegetation-atmosphere exchanges of carbon dioxide, and associated fluxes of water vapor, radiation and heat. With only a few direct long-term measurements of terrestrial carbon exchange available, these estimates are virtually unconstrained by reliable benchmark values (Baldocchi et al., 1996, and other papers in the same special issue). If, as the '*missing sink*' argument implies (Tans et al., 1990; Ciais et al., 1995; Schimel, 1995), mid-latitude forests play an important role in global carbon sequestration, its causes, dynamics, and future trends are unknown, leaving the potential for error in predictions of future atmospheric CO_2 concentrations wide open. Recently, the attribution of the *missing sink* to mid-latitude forests has gained support by linking satellite-inferred

* Corresponding author. Tel.: +1-812-855-6303;
fax: +1-812-855-1661.
E-mail address: hschmid@indiana.edu (H.P. Schmid)

increases in normalized difference vegetation index (NDVI) over the period 1981–1991 to net increases in biomass (Myneni et al., 1997). Another study reported an annual carbon sink over the north-eastern United States that alone accounts for the global missing sink, based on the carbon mass-balance inversion method for 1988–1992 (Fan et al., 1998). While these studies provide invaluable information about the magnitudes involved in the global carbon cycle, the large uncertainties in their results point to the deficiency of current knowledge about terrestrial carbon exchanges.

These concerns formed the basis for the establishment of long-term carbon flux networks in Europe (Euroflux, Valentini et al., 1996) and in the Americas (AmeriFlux, Wofsy and Hollinger, 1997). Together with other emerging networks in Australia and Asia, these efforts are coordinated by FLUXNET (Baldocchi et al., 1998). The flux measurements at MMSF, described in this study, are part of the AmeriFlux network and became operational in February 1998. This project concentrates on micrometeorological aspects of forest-atmosphere exchange. It is closely associated and complemented by partner projects on ecosystem responses to carbon exchange, and on carbon–nitrogen relations (Pryor et al., 1998; Randolph, 1998).

To gain process level knowledge on forest-atmosphere exchange of carbon dioxide, it is necessary to recognize the linkages between the exchange of carbon, water vapor, heat and radiation. In this paper, we discuss daily and seasonal variations of exchanges of energy and carbon dioxide using the framework of the surface energy balance equation

$$Q^* = Q_H + Q_E + Q_G + \Delta Q_S + Q_P \tag{1}$$

where Q^* is the net radiation, Q_H and Q_E the fluxes of sensible and latent heat, respectively, Q_G the soil heat flux, ΔQ_S the heat storage change in the canopy volume and Q_P is the energy fixed by photosynthesis), and a simplified form of the ecosystem carbon balance equation

$$NEP = GEP - R_E = -(F_{CO_2} + \Delta C_S) \tag{2}$$

where NEP is the net ecosystem production, GEP the gross ecosystem production due to photosynthesis minus plant respiration, R_E the total ecosystem respiration, F_{CO_2} the net flux of carbon dioxide and ΔC_S is

the carbon storage change in the volume. The symbol Q_E and the term 'evaporation' are used synonymously with 'evapotranspiration'. For atmospheric fluxes, the usual sign convention, positive upward, is used. Thus, net ecosystem exchange, NEE=−NEP.

A detailed description of the methods and locations of measurement used for individual terms of these balance equations is given in Section 2. Data for time periods when measurements are missing due to precipitation, instrumentation problems or conditions in which the eddy covariance method becomes questionable for measuring the flux exchange (e.g., extremely weak turbulence in the stable boundary layer during calm nights) are interpolated using a simple parametric model, based on measurements of soil temperature and photosynthetically active radiation (PAR) (Section 4.3). Additional complications are introduced by the presence of topography and ensuing mean vertical flow components. Questions and concerns about the consequences of vertical mean flow, advection and instationarity on the form of the conservation of mass equation are addressed by Lee (1998), Paw U et al. (1998) and Finnigan (1999). The estimates from this study of annual carbon sequestration (net ecosystem production), annual gross ecosystem production and annual ecosystem respiration are discussed in terms of the magnitudes, uncertainties, and inter-annual variability found at other mid-latitude broad-leaf forest sites.

2. Site and instrumentation

MMSF, south-central Indiana (39°19′N, 86°25′W), 275 m a.s.l., is an extensive managed forest with a total area of 95.3 km². This area has a ridge/ravine topography with a relative relief of <60 m, and an overall drop of 90 m in 4 km. The area is covered primarily by a secondary successional broadleaf forest within the maple-beech to oak-hickory transition zone of the eastern deciduous forest (Braun, 1959; Barrett, 1994; Von Kley et al., 1994). Randolph (1998) and Ehman (personal communication), based on the basal areas from a survey of all trees with a diameter at breast height of ≥7 cm in 54 large plots (150 m² each) in the immediate vicinity of the tower, identified 29 species, nearly 3/4 of which were sugar maple (*Acer saccharum*), tulip poplar (*Liriodendron tulipifera*), sassafras (*Sassafras albidum*), white oak (*Quercus alba*), and

Table 1
Species composition of tree basal area of MMSF from 54 large plots surrounding the study site covering a total of 8100 m². Total above ground biomass was determined as 19.52 kg m^{-2} (Ehman, personal communication)

Species	Basal area (m² ha^{-1})	Total (%)
Sugar maple (*Acer saccharum*)	7.14	27
Tulip poplar (*Liriodendron tulipifera*)	5.05	19
Sassafras (*Sassafras albidum*)	2.49	9.5
White oak (*Quercus alba*)	2.37	9.0
Black oak (*Quercus nigra*)	2.25	8.5
24 Other species	7.04	27
Total	26.34	100

black oak (*Quercus nigra*) (Table 1). The mean canopy height of the forest is ≈25–27 m. This forest is located just south of the limit of the Wisconsinan glaciation.

The study site is located so that the minimum fetch of essentially uninterrupted forest exceeds 4 km in any direction, and reaches up to 8 km in the principal wind direction (westerly to south-westerly). The principal site for flux measurements is a 46 m meteorological tower (Fig. 1), which is accessed via a non-public road. These measurements are augmented by four micrometeorological stations below canopy in the expected footprint of the tower.

Observations of vegetation area index (VAI) are taken periodically over the vegetative season along three transects (10 locations each) in the north-western, western and south-western directions (Fig. 1). The MMSF flux tower is a self-supporting structure of hot-dipped zinc galvanized steel with a triangular cross section. The height of the upper-most instrumentation level is 45.7 m (=1.76 times the canopy height). The tower has a base of 5.1 m side-length and tapers to 1.8 at 30.5 m. The top 15.3 m is vertical with uniform triangular cross-sections. The tower is equipped with an interior ladder and six full steel grid work-platforms every 6 m from the top. A climatized equipment shelter (5.5 m×2.5 m), with telephone and power, close to the tower base houses the data
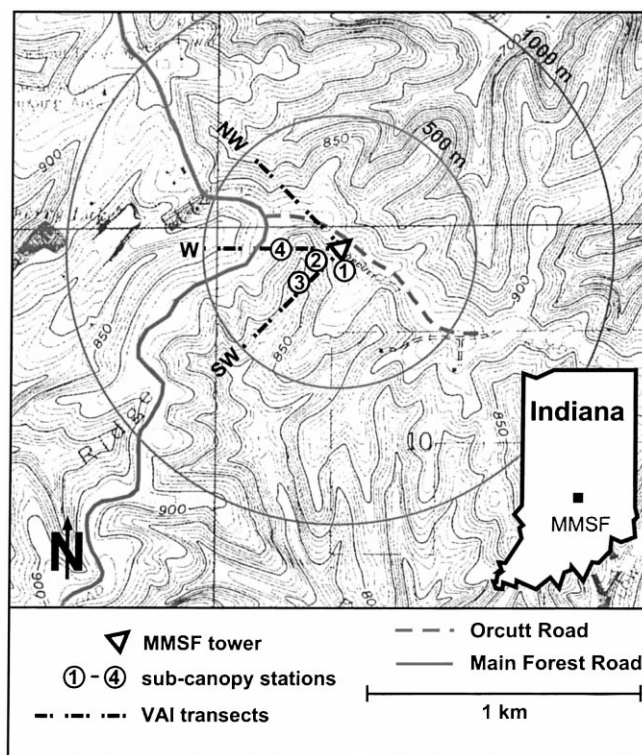

Fig. 1. Map of the MMSF tower site. Contour interval is 10 ft (3.05 m).

acquisition equipment, the gas flow control system, and the Infra-red gas analyzers (IRGAs, Li-6262 from LiCor, Lincoln, NE).

The micrometeorological instrumentation is organized into two main observation levels for flux measurements on the tower (at 46 and 34 m) and one on a separate mast below canopy (at 1–2 m). The latter is ≈10 m to the southwest of the tower, to avoid the disturbance in the canopy structure created by the tower (see Table 2 for a summary of all instrumentation). At each of these levels the four components of the radiation balance are measured separately, along with net all wave radiation (Q^*), and sensors for PAR are located at 46 m, at 22 m (≈80% of canopy height), and at 2 m, below canopy. Total incoming shortwave radiation ($K\downarrow$) is also measured at approximately canopy height (28 m), in mid-canopy (14 m), and again at 2 m, to complete a six level profile of incoming shortwave radiation ($K\downarrow$ or PAR) through the canopy.

Measurements of three dimensional turbulent velocity fluctuations and eddy-covariance fluxes of

momentum, sensible heat, water vapor, and CO_2 are also obtained at 46, 34, and 2 m. At the two above-canopy levels, the azimuth orientation of the sonic anemometers is 230°. The fluxes of momentum and heat are evaluated directly from the three-dimensional sonic anemometers (CSAT, Campbell Scientific Inc. (CSI), Logan, UT, 10 Hz sampling rate). The water vapor and CO_2 concentrations are measured by pumping sample air from the three sonic anemometer levels to individual closed-path IRGAs inside the shelter. Eddy-covariance fluxes are then obtained during post-processing (Section 3).

These flux levels are augmented by profile measurements of CO_2, air temperature and relative humidity at multiple levels above and throughout the canopy. Detailed profiles of water vapor and CO_2 mixing ratio profiles are obtained by cycling through eight levels of air intake tubes, using a computer-controlled solenoid-valve manifold in conjunction with an IRGA. The intake tubes of the lower seven levels (below canopy, Table 2) are suspended between two large

Table 2
Instrumentation for continuous micrometeorological observations at the MMSF tower[a]

	Measurement	Manufacturer	Instrument
Fluxes			
46, 34, 2 m	3D Wind, eddy-covariance	CSI, Logan, UT	CSAT
46, 34, 2 m	CO_2 and H_2O, eddy-covariance	LiCor, Lincoln, NE	Li-6262
46, 34, 2 m	Four component net radiation	Kipp and Zonen, Bohemia, NY	CNR1
46, 34, 2 (4×) m	Net radiation	REBS, Seattle, WA	Q^*7/Q^*6
28, 14, 2 (4×) m	Incoming short wave	LiCor, Lincoln, NE	Li-200SZ-50
46, 22, 2 (4×) m	PAR	LiCor Lincoln, NE	Li-190SZ-50
Profiles			
32, 16, 8, 4, 2, 1, 0.5, 0.25 m	CO_2 and H_2O, mean profile	LiCor Lincoln, NE	Li-6262
(32×)	Bole temperature	Omega, Stamford, CT	T-type
46, 34, 22, 12, 6, 1 m	Air temperature and relative humidity	Vaisala (sensors), Woburn, MA	HMP35C
		R.E. Young (shields), Traverse City, MI	(Aspirated)
Auxiliary			
0 m	Barometric pressure	Vaisala, Woburn, MA	PTA 427
46, 0 (4×) m	Precipitation	Texas Electronics, Dallas, TX	TE525
		Qualimetrics, Sacramento, CA	6011-B
3 m	Snow depth	CSI, Logan, UT	SR-50
Soil			
(6×)	Surface wetness	CSI, Logan, UT	237
(4×)	Soil moisture	CSI, Logan, UT	CS615
(4×)	Soil temperature	Omega, Stamford, CT	T-type
(4×)	Soil temperature	CSI, Logan, UT	TCAV
(8×)	Soil heat flux plates	REBS, Seattle, WA	HFT

[a] Multiple sensors distributed in the study area are indicated by their number (e.g., 4× or 32×).

trees, so that they are located within undisturbed canopy space. Air temperature and humidity profiles are provided by six levels of combined ventilated T/RH probes along one leg of the tower (Table 2). To evaluate the heat storage dynamics of tree trunks and boles in the canopy volume, a number of trees of various species and stages of maturity have been equipped with bole temperature sensors. These profile measurements form the basis for the evaluation of the canopy volume storage terms of heat and CO_2 in Eqs. (1) and (2). All these variables are sampled at 10 Hz and pre-processed by a National Instruments Inc. (Austin, TX) data acquisition unit with LabView software.

Below-canopy conditions are examined by four micrometeorological stations distributed within the expected footprint of the tower measurements. Variables measured at these stations include Q^*, PAR, soil moisture, soil temperature, soil heat flux (Q_G), and precipitation. At the main below-canopy station (co-located with the 2 m eddy-covariance station), surface wetness and snow depth also are measured. The other three micrometeorological stations are co-located with three of the ecological plots (Fig. 1). These micrometeorological variables are sampled at 5 s and averaged to 30 min by CSI 21X data loggers.

3. Eddy-covariance data acquisition and processing

3.1. Overview

The main instruments used for the eddy-covariance system are a CSAT 3-D sonic anemometer and an IRGA for each level (Table 2). Sample gas is pumped from the intake near the sonic anemometer array to the IRGA through Teflon tubing with an inner diameter of 4.8 mm. The total line length for the 46 m measurement level amounts to nearly 60 m. Inline Teflon filters (Gelman Inc., pore size=1 μm) near the gas intake prevent dust and dirt from entering the tubing. Heating tape, applied to the tubing on both sides of the filters and to the filters themselves, prevents the pressure drop associated with filtration from causing condensation. Inside the shelter, another section of the Teflon tubing is heated to damp out temperature fluctuations in the gas, and to allow the IRGAs to operate

at conditions of constant temperature. A further filter in the tubing immediately before the IRGA intake protects the optical bench of the IRGA from any residual contamination. On the exhaust side of the IRGA, the flow rate is monitored by a mass flow controller (GFC-17S, Aalborg Inc., Orangeburg, NY). This is connected in turn to a diaphragm pump, after passing through a dead volume, to dampen out vibrations from the pumps. The flow rate is approximately $7.5 \, l \, min^{-1}$, leading to a Reynolds number of the flow of around 2300, just above the turbulence limit. The transit time for the 60 m tubing is on the order of 6–7 s.

3.2. IRGA and eddy-correlation data processing

Calibration of the gas analyzers against gas standards that are traceable to the National Institute of Standards is done at sampling pressure and flow rate to reduce the dependence upon the corrections applied using the IRGA's internal pressure transducer cell. A system of solenoid valves enables gas cylinders for IRGA calibration to be permanently connected: the fixed connections decrease the susceptibility of the system to contamination by leaks. One solenoid valve in each of the sample lines switches between 'line gas' (from the tower) and calibration gas, which derives from a manifold. A second solenoid valve controls the flow of nitrogen gas or calibration standard CO_2 to the manifold. Needle valves allow adjustment of flow and pressure conditions in the IRGA to be identical to measurement conditions. Valve settings need to be set manually when gas cylinders are exchanged. A set of (electrical) switches allows this system to be operated either manually or automatically by the logging system in a scheduled manner. Currently, the calibration system cycles over the four IRGAs automatically every 27 h, so that the time of day for the calibrations is incremented daily. Automatic calibrations monitor but do not alter the IRGA instrument calibration. A span gas for water vapor calibration is not available at high enough flow rate. It is our intention that H_2O span calibration be done by reference to a calibration humidity probe on the tower near the gas intake, though currently this is not done, except by weekly comparison with psychrometer readings.

Raw voltage values (mV) of CO_2, H_2O, sample cell temperature and pressure are recorded at a rate of 10 Hz. The mixing ratios (in mole fraction) of CO_2

and H_2O are then calculated following the procedures described in the manual of Li-6262 and calibration coefficients specific for each IRGA. These include the dilution correction due to water vapor (Webb et al., 1980). Eddy-covariance fluxes are calculated by shifting the time series of the gas concentration and vertical velocity to maximize the correlation coefficient between them. A first guess for the lag window is provided by the flow rate and the tube dimensions.

Detection and rejection of data spikes is achieved during data processing of both the IRGAs and the sonic anemometers, using a conservative approach. Some spikes are indicated by a flag variable in the CSAT output, indicating problems, such as a blocked path between a sensor pair. Such flagged spikes can generally be attributed to precipitation. Following Vickers and Mahrt (1997), we call these 'hard' spikes and unambiguously reject the corresponding periods of CSAT data. This is a conservative policy as some of the CSAT flag values indicate that the data is merely suspect and not unusable outright.

A second type of spike, termed here 'soft' spikes because they are detected by post-processing criteria, are large short-lived departures from the (15 min) means, detected in an iterative process, similar to that described in Højstrup (1993) (although his model applies to the time derivative of the signal). For each 15 min period and variable, the means and variances are calculated. From these diagnostics, a threshold for spikes is determined as a multiple of the standard deviation, with the multiplier increasing on each iteration (3.6 S.D. initially, increased by 0.3 after each pass). On each pass, a soft spike is registered if the fluctuation from the mean is larger than the threshold value, and if the duration of the spike is three or fewer records, corresponding to a persistence of 0.3 s for the 10 Hz sampling rate. Longer-lasting departures from the period mean are taken to indicate possible physical events. After each pass, if spikes are detected, the mean and variance are adjusted to exclude data marked as spikes and the process repeated, until either there are no more new spikes or the maximum of three iterations is completed (which is rarely the case).

It was found that hard and soft spikes are closely related. The data appear to start to go out of range before the instrument's self-diagnosis indicates a problem, which vindicates the decision to take a conservative approach to data rejection. After this first phase of quality control, eddy-correlation fluxes and other turbulence statistics are determined over periods of 15 min, if more than 50% of the raw data pass the spike rejection test for a given 15 min block. Otherwise, the entire block is treated as a missing value. Here, traditional Reynolds decomposition based on block averages is used, although this method requires an assumption of weak stationarity, which is unlikely to be strictly warranted in all conditions encountered during the study period (e.g., Paw U et al., 1998).

In a second phase of quality control, all measured or derived variables (15 min averages) are submitted to a plausibility test and are rejected if they fall outside statically defined constraints for each variable (e.g., energy fluxes not to exceed the solar constant, CO_2 fluxes not to exceed $\pm 50\,\mu mol\,m^{-2}\,s^{-1}$). Subsequently, the 15 min data are reduced to hourly averages. If more than one 15 min block in a given hour is missing, the entire hour is treated as a missing value.

The use of three or four 15 min block averages for hourly fluxes over very rough surfaces is a strategy to minimize the need to reject data over a given measurement period. It is a compromise between including the peak frequencies of the co-spectrum and avoiding non-stationarity effects in longer averaging periods, but raises the question of unresolved flux contributions at periods longer than 15 min. On YD 98/175–177 (24–26 June 1998), a field comparison of the present eddy-covariance configuration and the AmeriFlux roving standard system, using 30 min flux averages but similar tubing and flow rate, was carried out (Evans, personal communications). For a description of the roving standard system, see http://cdiac.esd.ornl.gov/programs/ameriflux (Hollinger, personal communications). The results fully support the use of the present data management strategy. Measurements were conducted over a range of $12\,\mu mol\,m^{-2}\,s^{-1} \geq F_{CO_2} \geq -32\,\mu mol\,m^{-2}\,s^{-1}$. The F_{CO_2} values of the resident system at MMSF agreed very closely with the roving standard, as demonstrated by the regression statistics. Based on 86 observations, the coefficient of determination R^2, was 0.97 and the S.E. $1.8\,\mu mol\,m^{-2}\,s^{-1}$. The MMSF system overestimated the roving standard slightly, with a slope of 1.08. For H_2O, the comparison was even more favorable, with a slope of 1.003 and an R^2 of 0.99. From this comparison, we conclude that the use of 15 min windows for flux calculations did not lead to

an underestimation of the flux, compared to using a 30 min window, but reduced the need to reject data considerably.

3.3. Frequency response of CO_2 and H_2O measurements

Although the Li-6262 CO_2/H_2O IRGA allows a 10 Hz sampling rate, the actual frequency resolution of CO_2 and H_2O measurements is likely reduced by any mixing or smearing of the sampled ambient air in the long tube of 60 m, through which the sample air is pumped. To correct flux measurements for such tube attenuations, various methods have been suggested (e.g., Moore, 1986; Leuning and Moncrieff, 1990; Eugster and Senn, 1995; Leuning and Judd, 1996; Massman, 2000) with differing degrees of assumptions about the corrected shape of the spectrum. We consider this topic a research question that needs careful consideration where individual values of measured fluxes are important. Here, we concentrate on relative magnitudes and argue that, for the present method to obtain an annual estimate of NEP, the effect of tube attenuation is small.

In samples of spectra from the measured CO_2 and H_2O time series (not shown), the $-5/3$ slope of the inertial subrange only extends to a natural frequency of about 0.1–0.2 Hz, above which the spectral densities decay with an increasing slope, and are reduced to the white noise level above 1 Hz (the actual IRGA resolution limit for our configuration). This finding is no surprise, because the tube acts as a low-pass filter and higher frequencies are attenuated more effectively. The strength of this attenuation depends on the Reynolds number, on the tube diameter, the tube material and on its length. The residence time in the tube is approximately equivalent to the time constant of the tube attenuation characteristics (Eugster and Senn, 1995). As shown by Leuning and Moncrieff (1990), the relative magnitude of the flux loss due to tube attenuation depends upon the mean wind speed and measurement height, in addition to the tube attenuation characteristics.

However, for the present purposes of analyzing data from the 46 m level, spectral losses are considered minimal. This conclusion is reached, because (i) large organized coherent structures dominate the exchange over tall forest canopies (Shaw and Tavangar, 1983;

Raupach et al., 1986; Su et al., 1998) with a spatial length scale of 4–12 times canopy height (Zhang et al., 1992; Raupach et al., 1996; Su et al., 2000), and (ii) the eddy-covariance system at 46 m is relatively high, corresponding to about 1.8 canopy heights, so that the percentage of flux correction is expected to be small. For example, Leuning and Moncrieff (1990) showed that, for a mean wind speed range from 1 to 10 m s^{-1}, flux loss ranged from 21 to 38% at 1 m height, the corresponding loss for 8 m height is reduced to between 4 and 8%. For our measurement height at more than 25 m above the displacement level, we expect substantial further reduction of this effect.

Our assessment of the minimal impact of tube attenuation for our experimental design and data treatment is confirmed indirectly by an independent estimate of annual NEP, from measurements of above and below ground biomass increments (Ehman et al., 1999), within 10% of the micrometeorological flux integration value, as presented in Section 5.

4. Results

4.1. Micrometeorological site characterization

The albedo (α) of the tower site was determined with the up- and down-looking CNR1 pyranometers at 46 m (Fig. 2a). To avoid run-away ratios and low solar angles, only hourly couplets with incoming shortwave radiation, $K\downarrow$>150 W m^{-2} were used. During the initial period of foliage development, up to 98/140 (20 May), albedo increased quickly from 0.11 to almost 0.17. In the rest of the growing season (late May to late August), α decreased gradually. This could be attributed to: (i) increased leaf darkness with senescence; and (ii) continuing growth of foliage, trapping more radiation via multiple reflection inside the forest (Jones, 1992). However, there is no clear evidence of significant increase in VAI (Fig. 2b) from late May to early September. The slight increase in α after about 98/260 (17 September) may represent the bright fall coloration of the foliage, before a sharper decrease back to the leaf-off level in November (after 98/305). The average leaf-on value of α (0.15$\pm$0.02) is relatively low for deciduous forests (Oke, 1987; Garratt, 1992).
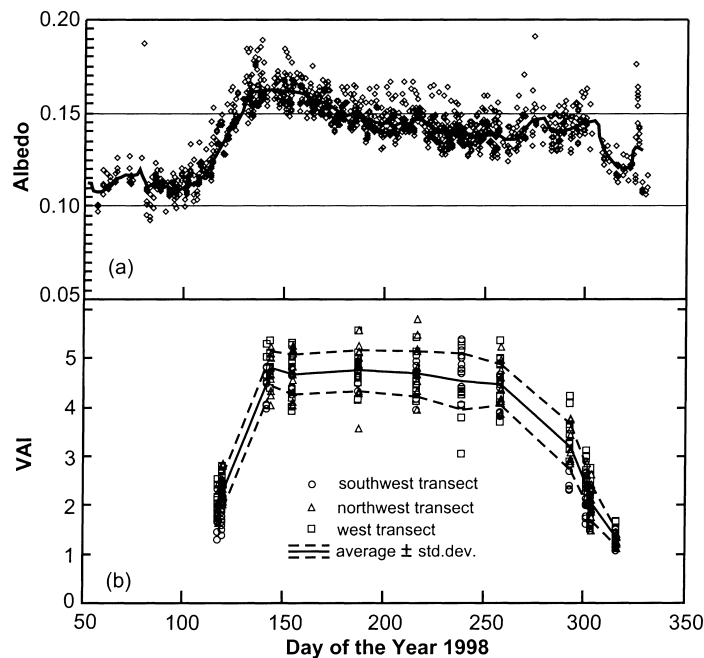
Fig. 2. Forest phenology over the vegetative season of 1998 at MMSF. (a) Variation of albedo. Dots are hourly values and the solid line is a 10 day moving average. (b) Evolution of total VAI. See Fig. 1 for transect locations.

Total VAI was measured periodically at over 30 locations on three transects in south-western, north-western, and western direction, using a LiCor LAI-2000 sensor, with full sky reference measured at the top of the tower (Fig. 2b). The leaf-off bole area index was determined at about 1.3±0.16 on 13 November (98/317), after leaf fall. Unfortunately, adverse weather conditions in spring of 1998 prevented most VAI measurements during the budding period, starting in early April. Because the winter of 1997–1998 was unusually mild in this region (mostly attributed to the strong El Nino event during that period), the onset of budding was visually observed to be about 2 weeks earlier than usual (Randolph, personal communication). The data show that this period was complete by 22 May (98/142), after which VAI remained approximately constant at 4.7±0.5 until 98/217, at the beginning of August. In August and the first half of September, leaf senescence decreased the VAI to 4.48±0.4, and after that date (98/259) the foliage began to fall, as indicated by the steepening decrease of VAI down to its leaf-off value. The magnitudes and evolution pattern of VAI at the MMSF

site are very similar to those for the oak-hickory forest at the Walker Branch AmeriFlux site near Oak Ridge, Tennessee, as reported by Huchison et al. (1986) and more recently by Greco and Baldocchi (1996), forthwith denoted as GB96 for the vegetative season of 1993. Due to the latitudinal difference (Walker Branch is at 35°57′N, 3°22′ further south than MMSF), we expect that the growing season at Walker Branch is typically longer than at MMSF, as direct phenological comparisons confirm (Baldocchi, 1999, personal communication).

To estimate the roughness length of the forest (z_0), the hourly values of mean wind speed and friction velocity measured by the sonic anemometer at 46 m were used for near neutral conditions (where $|L| > 1000$ m, and L is the Obukhov length) with wind speeds over $2\,\mathrm{m\,s^{-1}}$, in conjunction with the logarithmic wind profile relation. It was assumed that the zero-plane displacement height, $z_d = 0.8h$, where h is the mean canopy height of 26 m. Changing z_d to $0.75h$ affected the computed roughness lengths insignificantly. The mean value was computed to be $z_0 = 2.1 \pm 1.1$ m. This value is surprisingly constant

with wind direction around the site, except for a narrow sector at about $50°$, where the apparent z_0 decreases to nearly 1 m. Flow reaching the sensor from this sector comes across the broad ridge on which the tower is located (Fig. 1), but this sector also is aligned with the tower structure upwind of the sensor, thus flow conditions are very likely disturbed. There is no discernable seasonal variation between leaf off and leaf out periods. The use of the logarithmic wind profile relation is not a priori warranted here, because the 46 m level may be too low to be above the roughness sub-layer, where the logarithmic law does not apply. In addition, terrain induced flow features would need to be considered in a more exact analysis. However, the relatively well-behaved results (not shown) justify the use of this crude method for an estimate of z_0.

4.2. CO_2 and energy fluxes: daily and seasonal variations

Despite the good agreement of the present eddy-covariance system with the AmeriFlux standard, the data available at this time do not allow detailed interpretations of the energy balance in the soil-canopy-air volume at this site, before some of the concerns associated with topographic effects and divergence, mentioned in the introduction can be addressed. In addition, the spatial representativeness of the radiation and eddy-covariance footprints need to be examined (Schmid, 1997). Using the present data, and assuming that total Q_G is small on an annual basis, the annual totals of $Q^* - (Q_H + Q_E) = Q^* \times 17\%$. This lack of closure is large, but comparable to similar studies (Blanken et al., 1998). Thus, our emphasis here is not on absolute values of energy fluxes, but on the diurnal and seasonal patterns.

Because of their multiple links to the ecophysiology of the forest, the seasonal and diurnal patterns of radiation, sensible heat, evaporation and carbon fluxes need to be examined in concert. These results are presented in Figs. 3–5b. Even without complete confidence in the absolute levels of Q_E and Q_H, Figs. 3 and 4 demonstrate the close link between net radiation and the turbulent fluxes. However, whereas
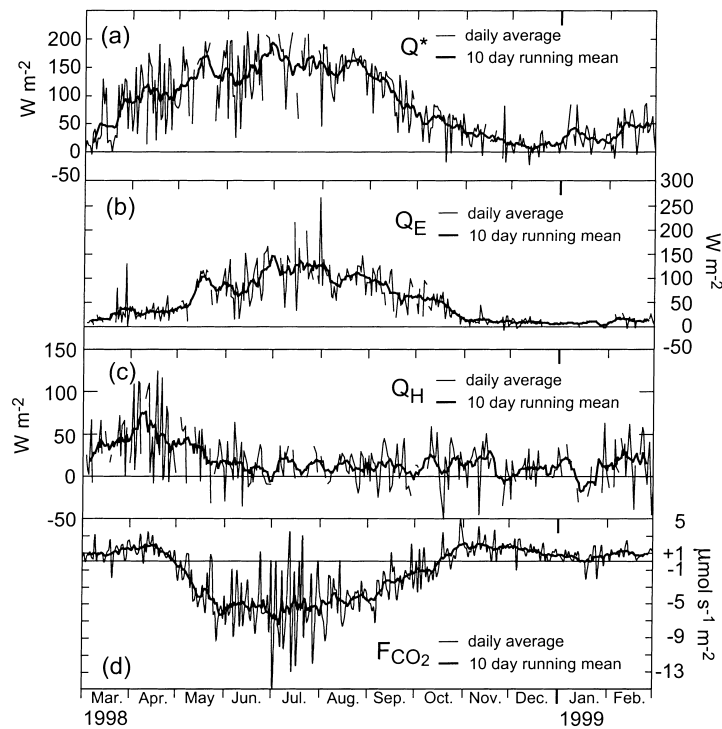

Fig. 3. Annual variation of energy and CO_2 fluxes: (a) net radiation; (b) latent heat; (c) sensible heat and (d) CO_2.
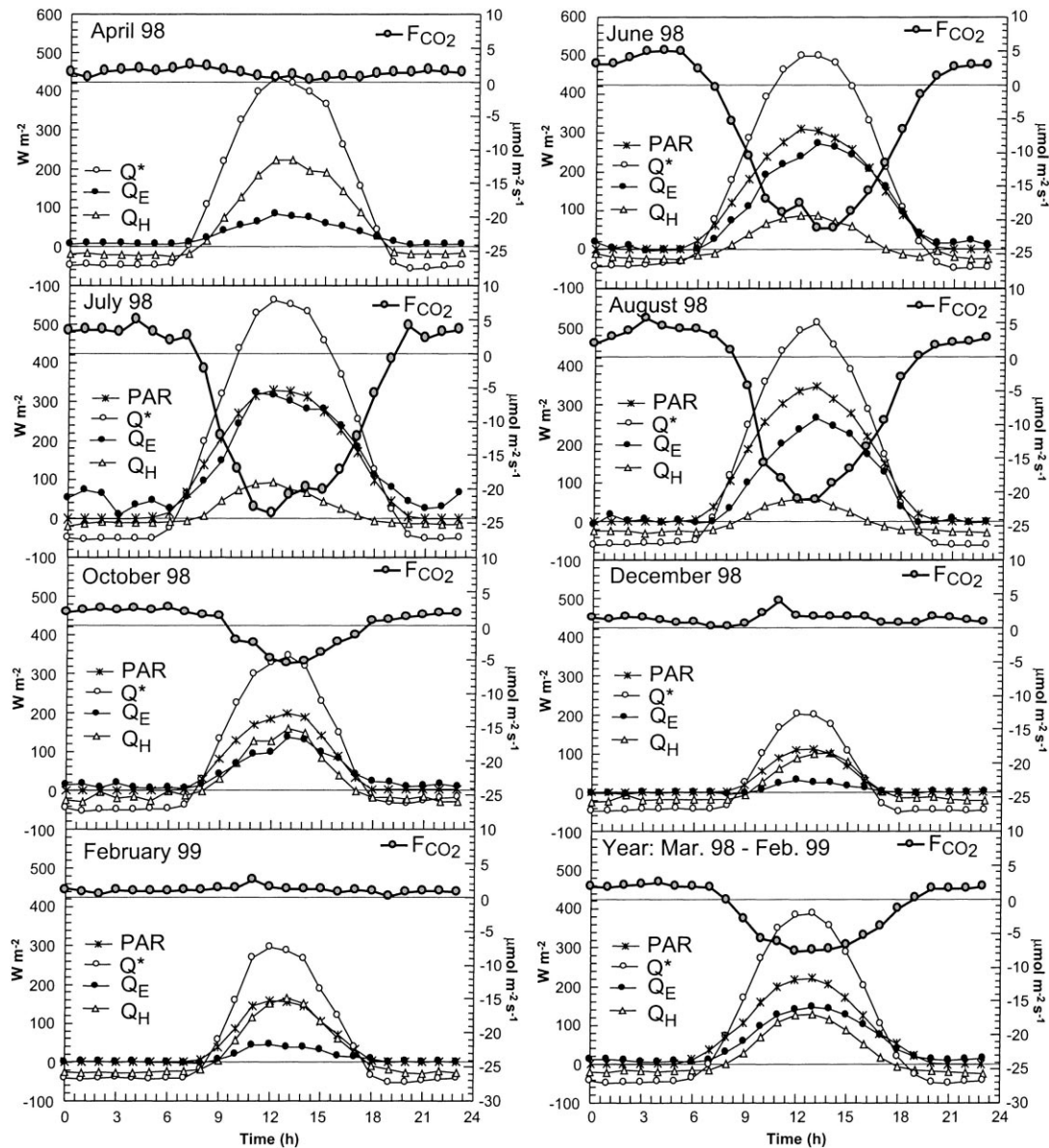
Fig. 4. Ensemble mean daily cycles of energy and CO_2 exchange for April, June, July, August, October, December 1998, February 1999, and for the entire year.

Q_H follows the course of Q^* closely in early spring, it starts to decay drastically at the end of April and becomes almost completely decoupled from net radiation by the end of May. This occurs because of increasing latent heat transport, driven by transpiration from the emerging forest foliage. This trend is reversed after leaf fall in October, when Q_E decreases and Q_H once again becomes more significant to the diurnal course of energy partitioning. Similar patterns have been observed at other sites (e.g., Blanken et al., 1997). The monthly mean diurnal variations (Fig. 4) confirm that during the vegetative period
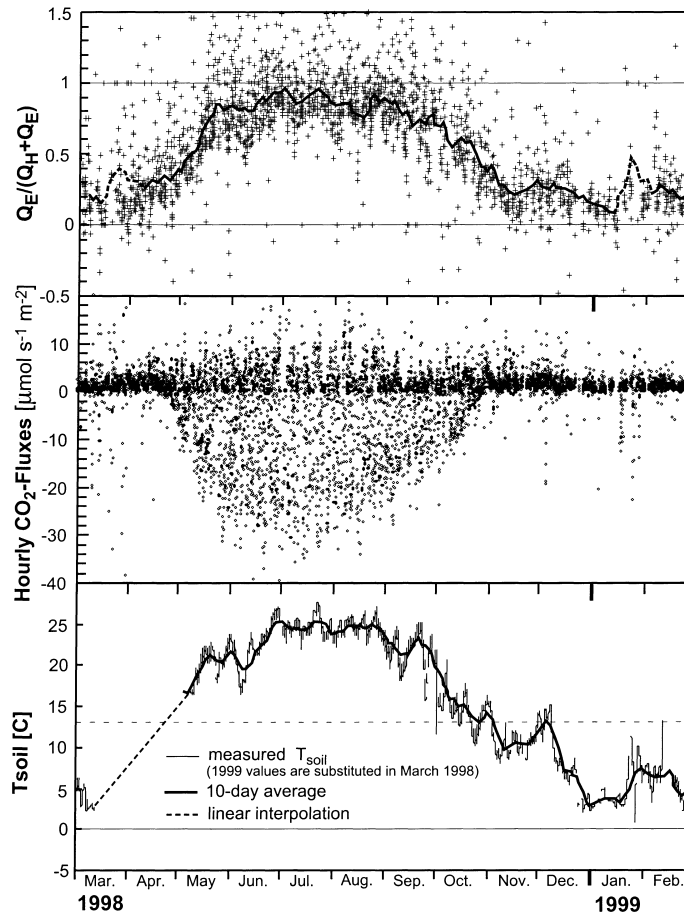
Fig. 5. (a) Annual course of day-time partitioning of convective energy at MMSF, 46 m level. Plus signs (+) are hourly ratios and the heavy line is a 10-day moving average. The dashed peaks indicate significant data gaps. (b) Annual composite of hourly CO_2 fluxes measured by eddy-covariance at 46 m above MMSF. Negative values indicate that the forest is a net sink of CO_2. (c) Evolution of soil temperature (at 5 cm) over the study period. Data for March and April 1998 are unavailable. The use of March 1999 data and an interpolation for the purposes of the GEP model is explained in the text.

the available energy is dominated by Q_E, while the sensible heat flux exhibits only a weak diurnal pattern. Between mid-May and mid-September, about 85% of the day-time ($K\downarrow > 100\,\mathrm{W\,m^{-2}}$) available energy is consumed by evaporation, in contrast to only around 20–30% during the leaf-off period (Fig. 5a). A comparison with Fig. 2b shows a strong correlation between energy partitioning and the development of VAI over the period. Grimmond et al. (2000) demonstrate that transpiration from trees and evaporation of intercepted precipitation by the forest canopy contribute about 90% of the measured H_2O flux above canopy during the growing season. However, their

measurements indicate that evaporation of intercepted precipitation dominates transpiration by roughly 25%.

The amount of PAR incident on the canopy, during the period when VAI is at its maximum, closely matches the amount of latent heat consumed during the day (Fig. 4). This relationship is quite distinct for June and July and to a lesser extent for August (August 1998 was very dry). Daily total evaporation at a similar forest site in the Walker Branch Watershed, TN, reported by GB96 for the year 1993 shows similar magnitudes of Q_E to the present study. On the one summer day (YD 244, 1 September) reported Q_E reached only about 75% of PAR, but the authors note

that the forest exhibited signs of water stress during that time.

As expected, the close physiological link between leaf transpiration and the net exchange of CO_2 above the canopy is expressed clearly both in the seasonal patterns and their diurnal course (Figs. 3 and 4). Negative values of F_{CO_2} are directed towards the forest and signify photosynthetic activity. Consistent with the rapid development of VAI in April and May, day-time negative CO_2 fluxes show a sharp gradient during this period. While respiration is still dominant throughout the monthly mean day in April (Fig. 4), with hardly any organized diurnal pattern in the net flux, the forest has clearly become a net carbon sink in May (Figs. 3d and 5b). Fig. 3d shows that measured daily average respiration rates are low during most of winter. With warmer temperatures in April, respiration rates increase to result in net exchange of about $5 \, \mu mol \, m^{-2} \, s^{-1}$ in the daily average, despite the onset of budding and photosynthetic activity. Peak positive hourly fluxes reach up to $10 \, \mu mol \, m^{-2} \, s^{-1}$ during this period (Fig. 5b).

The scatter in Fig. 5b is an expression of the diurnal and seasonal courses of F_{CO_2}, modulated by variations in weather conditions that affect F_{CO_2} through changes in the radiation balance, temperature, and moisture availability. However, small negative fluxes (and occasionally substantial ones) were obtained throughout the leaf-off period. This finding is consistent with the experience of other long-term flux observation sites over deciduous forests (e.g., GB96; Goulden et al., 1996a, forthwith G96). The persistence in the occurrence of the smaller negative values in Fig. 5b, and the relatively large magnitude of the episodic ones during the period when photosynthesis is absent, suggests that these measurements cannot simply be attributed to instrument error. For this reason, they are not a priori rejected in our estimates of net ecosystem exchange (see below). The attempt to partition these values into instrumental errors and CO_2 storage change in the soil-canopy-air volume beneath the tower, due to, for example, topographically induced episodic horizontal divergence, is a research question that will be pursued elsewhere. The short term and episodic nature of these negative fluxes is confirmed by the fact that they usually disappear in the monthly averages for the leaf-off period (Fig. 4). In December 1998 and February 1999, there is a hint of a diurnal pattern of increased

respiration rates around noon, whereas the beginning of photosynthesis is hinted at by the slight reduction of net exchange during mid-day in April 1998.

4.3. Annual net carbon exchange and a simple model

In principle, eddy-covariance measurements of F_{CO_2} at 46 m ($\sim$1.8 canopy heights) provide direct measurements of the net ecosystem production or exchange (NEP or NEE) over the course of the study period. The ensemble of hourly observations of net ecosystem exchange is shown in Fig. 5b. Net ecosystem production can be formulated as a balance of gross ecosystem production (GEP, consisting of carboxylation, photorespiration and dark respiration; Farquhar et al., 1980), ecosystem respiration (R_E), and storage change.

The integral quality of the NEP observations presented in this study can be assessed by examining this balance based on some first-order assumptions for a given ecosystem

1. GEP is dominated by photosynthesis and is primarily controlled by the photosynthetically active photon flux density (PPFD) or PAR received during the vegetative period;
2. The length of the vegetative season is the period over which the soil temperature (T_s) rises above a certain threshold level T_{sc};
3. Ecosystem respiration is largely controlled by the soil temperature; and
4. For extended periods of a few days to years, storage change of gaseous carbon dioxide in the soil-air volume beneath the tower is negligible.

The last assumption requires that, on an annual basis

$$NEP_a = -\int^a F_{CO_2} \, dt = GEP_a - R_{E_a} \qquad (3)$$

in modification to Eq. (2), where the subscript 'a' refers to annual.

The above assumptions give rise to a very simple model for NEP

$$NEP = GEP(PPFD, T_s | T_s > T_{sc}) - R_E(T_s) \qquad (4)$$

Once suitable relationships for GEP and R_E have been found, Eq. (4) can be evaluated based on measured soil temperatures and rates of PPFD. However, it must be remembered that the model can only be valid over extended periods of at least a day (Assumption 4).

The annual course of soil temperature is presented in Fig. 5c. Unfortunately, soil temperature was not available before May 1998. For this reason, the first 10-days of March 1999 values were used in conjunction with a linear interpolation up to the first measured values during the study period, to supply soil temperatures to be used in the model. To obtain a relationship between respiration and soil temperature, measured values of F_{CO_2} from the 46 m eddy-covariance system during the period when the canopy was not fully developed or off-leaf were used (excluding Days 98/142–259). This method is similar to that suggested by Wofsy et al. (1993) except that they used eddy-fluxes corrected for storage change which are not available for this site yet. To compensate for this, a criterion for the measured friction velocity $u_* > 0.5\,\mathrm{ms^{-1}}$ was applied to ensure well-developed turbulence and mixing between the sensor level and the soil surface. This criterion for u_* is more conservative than those suggested by G96 and Black et al. (1996) to exclude periods of intermittent turbulence, where the eddy-covariance technique becomes invalid. Based on chamber measurements and above-canopy eddy-covariance at Harvard Forest, Wofsy et al. (1993) determined that more than 80% of respiration is attributable to below-ground respiration (soil and root). Because the scatter in the results (Fig. 6) is very strong, the data were averaged in bins of 1°C width. An exponential function, similar to those proposed by the studies mentioned above (and others), was fitted to the bin-averages

$$R_{E} = 1.08 \exp(0.064 T_{s}) \qquad (5)$$

where the fluxes are in $\mu\mathrm{mol\,m^{-2}\,s^{-1}}$, and T_s is in °C. The strength of the linear relationship between modeled and observed fluxes (not the bin-averages) is expressed by a coefficient of determination (R^2)
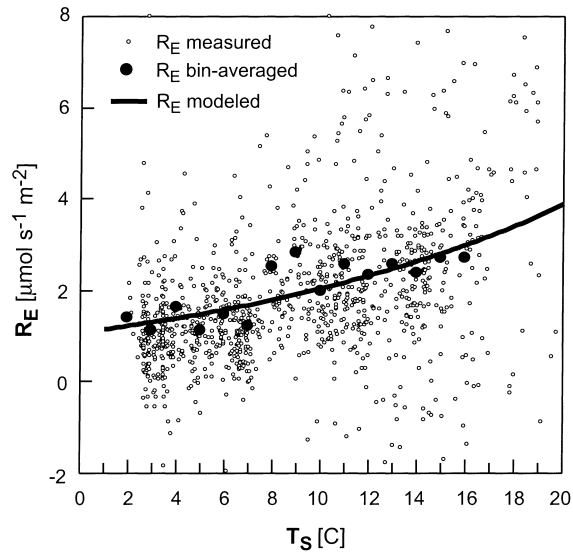

Fig. 6. Ecosystem respiration vs. soil temperature. The model (solid curve) fitted to the bin-averages is given in Eq. (5). ($R^2 = 0.66$).

of 0.66 ($n=1111$). The corresponding Q_{10} coefficient, the factor by which respiration increases with a rise of 10°C in soil temperature, is 1.89. This value lies well within those reported by various authors for other broadleaf forests (Table 3). Considering that the beech forest of Valentini et al. (1996) lies at an altitude of 1564 m a.s.l., Table 3 suggests a positive latitudinal trend of Q_{10} estimates for hardwood forests.

As postulated in Assumption (2), photosynthesis is fully active during a period when T_s remains above a certain threshold T_{sc}. A comparison of Figs. 2b and 5a and b with Fig. 5c supports this assumption and suggests a threshold temperature of $T_{sc}=13$°C, resulting in a vegetative period from the beginning of May to the end of October. As mentioned, this period corresponds well with direct phenological observations for

Table 3
Q_{10} values obtained for broadleaf forests (ordered by increasing value)

Forest	Location	Latitude	Source	Temperature	Q_{10}
Oak-hickory	Walker Branch, TN	36°N	GB96	Air	1.62
Maple-tulip poplar	Morgan-Monroe, IN	39°N	Present study	Soil	1.89
Oak-maple	Harvard forest, MA	42.5°N	G96	Soil	2.1
Beech	Central Italy, 1564 m a.s.l.	42°N	Valentini et al. (1996)	Air	2.17
Hardwood forests	Average worldwide	N/A	Kicklighter et al. (1994)	Soil	3.08
Boreal aspen	Prince Albert, Sask., CDN	53.7°N	Black et al. (1996)	Soil	5.4

1998. The same threshold temperature phenomenon, near the climatological average soil temperature, was observed also at other forests and for other years by Baldocchi (1999, personal communication). This finding suggests that the climatological average soil temperature may serve as a physiological or biochemical trigger for the vegetation.

Although Eq. (5) was obtained for a small subset of flux measurements (based on 12.7% of the data, see above), it was used to estimate gross ecosystem photosynthesis or GEP during day-time (PPFD>0), over the entire period when VAI was fully developed (from 22 May–16 September, 98/142–259, Fig. 2b), as the difference between $F_{CO_2} - R_E$, where R_E is obtained by Eq. (5). When the data are averaged to bins of 50 μmol m^{-2} s^{-1} of PPFD, the trend unrealistically shows no saturation at high PPFD (Fig. 7). Thus, the functional relationship fitted to the data was not allowed to adjust in a free regression. Instead, a similar equation to that used by G96 was used, allowing for saturation at higher PPFD values

$$\text{GEP} = -1.4 + 35 \times \frac{\text{PPFD}}{590 + \text{PPFD}} \qquad (6)$$

where the fluxes are in μmol m^{-2} s^{-1}. With Eq. (6) the maximum photosynthetic rate is estimated to be
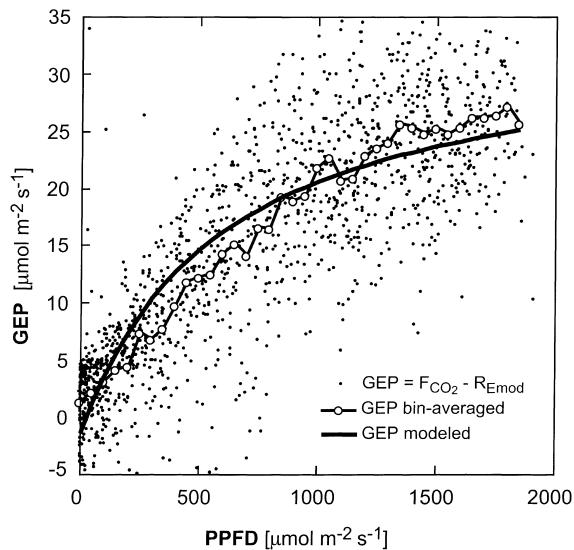

Fig. 7. GEP vs. PPFD. The model (smooth solid curve) is given in Eq. (6). (R^2=0.65).

slightly higher than at Harvard Forest (G96) and slightly lower than the theoretical optimum values for broadleaf forests proposed by GB96. The coefficient of determination between 'observed' and modeled GEP values using Eq. (6) is 0.65 (n=1466). In reality, this strong physical relation between radiation and photosynthesis is modulated by environmental factors affecting the vegetation, such as water stress and leaf area index (e.g., GB96), but these factors are ignored here.

Ecosystem respiration given by Eq. (5) was used to correct the net ecosystem CO_2 fluxes obtained by eddy-covariance during calm nights, when turbulence is not well developed or drainage effects may influence the measurements. In addition, the combination of Eqs. (4)–(6) was used to fill the data gaps in the F_{CO_2} time series over the entire study period. The cumulative NEE over the year (Fig. 8), arbitrarily starting at zero at the beginning of the study period, represents the raw time-integration of the 46 m eddy-covariance flux values. Because of the likely underestimation of night-time respiration by this method, and given the data gaps (apparent in Fig. 5b), the measured annual NEE estimate of 4.4 t C ha^{-1} is expected to be an overestimate. A corrected NEE was obtained by replacement of low-wind night-time periods ($u_* < 0.2$ m s^{-1}) eddy-covariance fluxes with R_E estimates from Eq. (5), and missing data were filled by the parametric model of Eq. (4), with Eqs. (5) and (6). The resulting curve of NEE corrected preserves most of the short term features of the measured fluxes, but reduces the annual carbon sequestration estimate to 2.4 t C ha^{-1}. In this scheme, the NEP model was applied 29% of the time (5.9% day-time data gaps, 23.1% night-time correction or data gaps). Total data gaps amounted to just under 16% of the time. If only the data gaps are filled with the parametric model, the cumulative NEE (the curve labeled 'NEE gap-filled' in Fig. 8) deviates only slightly from the measured curve, up to January 1999, when the system was down for several days.

As an alternative, the NEP model Eqs. (4)–(6) was used, based on measured values of T_s and PPFD throughout the year, in stand-alone mode (Fig. 8). Given the crudeness of this model, the qualitative and quantitative agreement with the corrected NEE observations is remarkable, because the parametric models use only a fraction of the data (12.7% for R_E, 16.7% for GEP). The annual sequestration obtained by the model
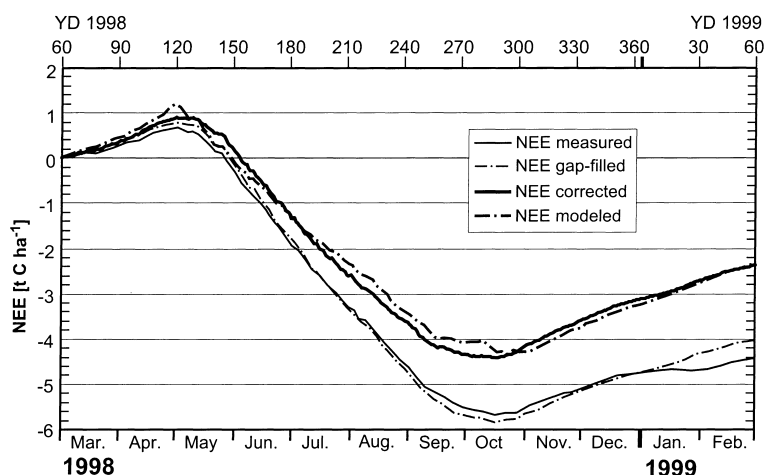
Fig. 8. Cumulative net ecosystem exchange (NEE) and annual carbon sequestration estimates using various degrees of assumptions. The NEE corrected curved is considered to be the most realistic estimate, leading to an annual carbon sequestration of 2.4 t C ha^{-1}. See text for details.

is 2.3 t C ha^{-1}, which is within 4% of the corrected observations. Of course, 29% of the corrected values depend on the model and are not completely independent from it. Thus, the value of the model (Eq. (6)) should not be overestimated. Here, the good agreement with the corrected observations is interpreted to confirm simply that, for a given forest and climatic setting, net ecosystem production is primarily controlled by (i) the amount of incoming radiation (PAR or PPFD), and (ii) soil temperature. The latter has a double role, as a direct indicator of the thermal environment for soil respiration, and as a threshold for vegetation activity.

5. Annual carbon sequestration and discussion

All four curves in Fig. 8 indicate an accelerating respiration rate in early spring, when temperatures were rising, but the forest foliage had not yet emerged. The curves also nearly agree about the date (1 May, for NEE corrected) when the forest became a net carbon sink again. This uptake of atmospheric carbon continued at an almost constant rate through to the beginning of September (mid-September in the model), when leaf senescence appeared to have an effect on GEP. The corrected observations estimate that, between May and mid-October, a total of 5.3 t C ha^{-1} were taken up by the forest (model estimate: 5.5 t C

ha^{-1}). Total net respiration during the off-leaf period was estimated as 2.9 t C ha^{-1}. The modeled annual GEP was 13.5 t C ha^{-1}, and the annual ecosystem respiration was determined as 11.1 t C ha^{-1}.

This result of 2.4 t C ha^{-1} per year (or 236 g C m^{-2} per year) of carbon sequestration in the first year of observation at this site reflects that MMSF is a managed forest. Although the most recent selective harvests in the vicinity of the tower were conducted at least 15 years ago (to the north), and more typically took place several decades ago, most of the forest is not fully mature. In addition, parts of the forest have suffered considerable damage from storms over the last few years, and are still recovering from that. Thus, it is expected that, even without further harvests, this forest has a considerable capacity to accumulate biomass for several years into the future. However, this sequestration value is a benchmark that needs to be examined closely and raises a series of questions for future research at this site.

The first question is how this value compares with directly measured sequestration estimates reported for other deciduous broadleaf forests in literature. The longest history of eddy-covariance measurements of CO$_2$ exchange exists for the Harvard Forest site. Wofsy et al. (1993) and Goulden et al. (1996b) report annual sequestration levels between 200–500 g C m^{-2} per year, suggesting a wide range of inter-annual

variability. GB96 obtained a net carbon uptake of $525\,g\,C\,m^{-2}$ per year for 1993–1994 at the Walker Branch site. Although they express some doubt about the quality of their night-time eddy-covariance measurements of CO_2, they were able to close the energy balance fairly well based on simultaneous eddy-covariance measurements of heat fluxes over this period. At the same site, Baldocchi et al. (1998) report a sequestration estimate for 1997 of $422\,g\,C\,m^{-2}$ per year, which is within 7% of their ecosystem exchange model. This value is derived after inclusion of a horizontal divergence–advection term, based on Lee (1998), to take account of night-time drainage flow induced by nocturnal cooling and topography. Without this correction, their estimate would amount to more than twice that value, because the correction term is important primarily during times when respiration is dominant. Sequestration estimates for 1994, 1996 and 1997 at the 70-years old Aspen site in Prince Albert (Black et al., 1996) are given by Chen et al. (1998) as between $140–180\,g\,C\,m^{-2}$ per year. If the night-time measurements are replaced by a soil temperature–respiration relationship for windy nights, similar to Eq. (5), their estimates are reduced by 40–50%. Thus, the $236\,g\,C\,m^{-2}$ per year of carbon sequestration for the MMSF site suggested here is on the same order of magnitude as the estimates published for other mid- to high-latitude deciduous forests. Direct comparisons for the same period are not yet available.

The second question addresses the uncertainty of this sequestration estimate. Using similar equipment and methods as in the present study, G96 estimate a long-term instrumental precision of the eddy-covariance measurements of $\pm 5\%$. However, as discussed in Section 4, systematic errors are likely to be dominant, primarily at times of poorly developed turbulence and mixing. The soil temperature based correction scheme used here suggests an underestimation of night-time (respiration) fluxes that affects the sequestration estimate by $\approx 50\%$, consistent with the findings for other sites and years. Fig. 6 illustrates that the data on which the correction scheme is based, contain a large amount of scatter, so that the correction scheme itself is subject to considerable uncertainty for hourly values. Over an annual integration interval the random parts of these uncertainties are likely to cancel, and thus, it is suspected that the remaining uncertainty in the annual sequestration estimate is largely

systematic, even after the soil temperature based correction. This could be due to several factors, including the inherent inability of a single flux tower to account for the volumetric mass balance in the soil-canopy-air volume (Finnigan, 1999), instationarity effects in the eddy-covariance time series (Paw U et al., 1998), transient flow effects associated with thermal circulations induced by topography or mesoscale inhomogeneities (Lee, 1998), and insufficient or inconsistent spatial representativeness of the radiation, eddy-flux and soil temperature measurements (Schmid, 1997). These uncertainties are common to most experimental sites where long term CO_2 exchange over tall vegetation is measured. However, because the processes that govern these systematic errors (and sometimes even their sign) are largely unknown themselves, we refrain from attempting a detailed analysis of the cumulative sequestration uncertainty here, other than that implied by the changing sequestration estimates under different sets of assumptions (Fig. 8). Based on these considerations, we estimate that the uncertainty of our annual sequestration estimate is on the order of 10%.

However, Ehman et al. (1999) computed the annual carbon sequestration rate for 1998–1999 based on ecological measurements of above and below ground biomass increments, and estimates of respiration from twenty $150\,m^2$ plots in the vicinity of the MMSF tower as $2.5\,t\,C\,ha^{-1}$ per year. The two estimates of NEP from micrometeorological and biomass increment measurements are completely independent, but lie within <5% of each other.

6. Conclusions

Based on the first full year of measurements (1998–1999) of above canopy CO_2 and energy fluxes at the AmeriFlux site in the MMSF, IN, USA, the following conclusions are drawn.
- The annual sequestration of atmospheric carbon by the mixed deciduous forest, between March 1998 and February 1999, is determined to be $2.4\,t\,C\,ha^{-1}$ per year. This estimate is based on eddy-covariance measurements above the forest, with a correction scheme based on soil temperature and PAR, to fill data gaps and replace measured fluxes during calm nights. An independent method to obtain

annual NEP by ecological measurements came to an estimate within 5% of this value. Net uptake of atmospheric carbon during the vegetative season amounted to $5.3\,t\,C\,ha^{-1}$ per year, and total net respiration during the off-leaf period returned $2.9\,t\,C\,ha^{-1}$ per year back to the atmosphere.

- This value of annual sequestration is estimated to be the result of $13.5\,t\,C\,ha^{-1}$ per year of gross ecosystem production and $11.1\,t\,C\,ha^{-1}$ per year of ecosystem respiration, based on a simple parametric model for respiration and GEP.
- The quantitative evaluation of the precision of such long term mass exchange estimates over tall vegetation involves the investigation of largely unknown flow phenomena induced by topography, or mesoscale inhomogeneity, and requires the development of new methodologies of micrometeorological experimental design to account for the entire mass balance in a soil-vegetation-atmosphere volume. Conclusive solutions to these problems are among the most pressing challenges that biosphere-atmosphere exchange research faces today.

References

Baldocchi, D.D., Valentini, R., Running, S., Oechel, W., Dahlman, R., 1996. Strategies for measuring and modelling carbon dioxide and water vapour fluxes over terrestrial ecosystems. Global Change Biol. 2, 169–182.

Baldocchi, D.D., Wilson, K., Paw U, K.T., 1998. On measuring net ecosystem carbon exchange in complex terrain over tall vegetation. In: Proceedings of the 23rd Conference on Agricultural and Forest Meteorology. American Meteorological Society, Boston, MA, Preprints, pp. 94–96.

Barrett, J.W., (Ed.) 1994. Regional silviculture of the United States. Wiley, New York, 643 pp.

Black, T.A., den Hartog, G., Neumann, H.H., Blanken, P.D., Yang, P.C., Russel, C., Nesic, Z., Lee, X., Chen, S.G., Staebler, R., Novak, M.D., 1996. Annual cycles of water vapor and carbon dioxide fluxes in and above a boreal aspen forest. Global Change Biol. 2, 219–229.

Blanken, P.D., Black, T.A., Yang, P.C., Neumann, H.H., Nesic, Z., Staebler, R., Den Hartog, G., Novak, M.D., Lee, X., 1997. Energy balance and canopy conductance of a boreal aspen forest: partitioning overstory and understory components. J. Geophys. Res. 102 (D24), 28915–28927.

Blanken, P.D., Black, T.A., Neumann, H.H., Den Hartog, G., Yang, P.C., Nesic, Z., Staebler, R., Chen, W., Novak, M.D., 1998. Turbulent flux measurements above and below the overstory of a boreal aspen forest. Boundary-Layer Meteorol. 89, 109–140.

Braun, E.L., 1959. Deciduous Forests of Eastern North America. The Blakiston Co., Philadelphia.

Chen, Z., Black, T.A., Barr, A.G., Yang, P.C., Chen, W.J., Nesic, Z., Swanson, R.V., Novak, M.D., 1998. Interannual variability of carbon dioxide and water vapor fluxes above a boreal aspen forest. In: Proceedings of the 23rd Conference on Agricultural and Forest Meteorology, American Meteorological Society, Boston, MA, Preprints, pp. 163–166.

Ciais, P., Tans, P.P., White, J.C., Francey, R.J., 1995. A large northern hemisphere terrestrial CO_2 sink indicated by the $^{13}C/^{12}C$ ratio of atmospheric CO_2. Science 269, 1098–1102.

Ehman J., Schmid, H.P., Grimmond, C.S.B., Hanson, P., Randolph, J.C., Cropley, F., 1999. A preliminary inter-comparison of micro-meteorological and ecological estimates of carbon sequestration in a mid-latitude deciduous forest. In: de Dear, R.J., Potter, J.C. (Eds.), Proceedings of the 15th International Congress on Biometeorology (ICB). Sydney, Australia, November 1999, ICBP03.06, 6 pp.

Eugster, W., Senn, W., 1995. A cospectral correction model for measurement of turbulent NO_2 flux. Boundary-Layer Meteorol. 74, 321–340.

Fan, S., Gloor, M., Mahlman, J., Pacala, S., Sarmiento, J., Takahashi, T., Tans, P., 1998. A large terrestrial carbon sink in North America implied by atmospheric and oceanic carbon dioxide data and models. Science 282, 442–446.

Farquhar, G.D., von Caemmerer, S., Berry, J.A., 1980. A biochemical model of photosynthetic CO_2 assimilation in leaves of C_3 species. Planta 149, 78–90.

Finnigan, J., 1999. A comment on the paper by Lee (1998) on micrometeorological observations of surface-air exchange over tall vegetation. Agric. For. Meteorol., in press.

Garratt, J.R., 1992. The Atmospheric Boundary Layer. Cambridge University Press, Cambridge, 316 pp.

Goulden, M.L., Munger, J.W., Fan, S.-M., Daube, B.C., Wofsy, S.C., 1996a. Measurements of carbon sequestration by long-term eddy-covariance: methods and a critical evaluation of accuracy. Global Change Biol. 2, 169–182.

Goulden, M.L., Munger, J.W., Fan, S.-M., Daube, B.C., Wofsy, S.C., 1996b. Exchange of carbon dioxide by a deciduous forest: response to interannual climate variability. Science 271, 1576–1578.

Greco, S., Baldocchi, D.D., 1996. Seasonal variations of CO_2 and water vapor exchange rates over a temperate deciduous forest. Global Change Biol. 2, 183–198.

Grimmond, C.S.B., Hanson, P.J., Schmid, H.P., Wullschleger, S.D., Cropley, F., 2000. Evaporation rates at the Morgan Monroe State Forest AmeriFlux site: a comparison of results from eddy-covariance turbulent flux measurements and sap flow techniques. In: Proceedings of the 15th Conference on Hydrology. American Meteorological Society, Boston, MA, January 2000, pp. 158–161.

Højstrup, J., 1993. A statistical data screening procedure. Meas. Sci. Technol. 4, 153–157.

Huchison et al., (1986) Jones, H.G., 1992. Plants and Microclimate — A Quantitative Approach to Environmental Plant Physiology, 2nd Edition. Cambridge University Press, Cambridge, 428 pp.

Kicklighter, D.W., Melillo, J.M., Peterjohn, W.T., Rastetter, E.B., Mcguire, A.D., Steudler, P.A., Aber, J.D., 1994. Aspects of spatial and temporal aggregation in estimating regional carbon-dioxide fluxes from temperature forest soil. J. Geophys. Res. 99 (D1), 1303–1315.

Johnes, H.G., 1992. Plants and Microclimate (2nd edn), Cambridge University Press, Cambridge, UK, 428 pp.

Lee, X., 1998. On micrometeorological observations of surface-air exchange over tall vegetation. Agric. For. Meteorol. 91, 39–49.

Leuning, R., Moncrieff, J., 1990. Eddy-covariance CO_2 flux measurements using open- and closed-path CO_2 analyzers: corrections for analyzer water vapor sensitivity and damping of fluctuations in air sampling tubes. Boundary-Layer Meteorol. 53, 63–76.

Leuning, R., Judd, M.J., 1996. The relative merits of open- and closed-path analyzers for measurement of eddy-fluxes. Global Change Biol. 2, 241–253.

Massman, W.J., 2000. A simple method for estimating frequency response corrections for eddy-covariance systems'. Agric. For. Meteorol., in press.

Moore, C.J., 1986. Frequency response corrections for eddy-correlation systems. Boundary-Layer Meteorol. 37, 17–35.

Myneni, R.B., Keeling, C.D., Tucker, C.J., Asrar, G., Nemani, R.R., 1997. Increased plant growth in the northern high latitudes from 1981–1991. Nature 386, 698–702.

Oke, T.R., 1987. Boundary Layer Climates, 2nd Edition. Methuen, London, 435 pp.

Paw U, K.T., Baldocchi, D.D., Meyers, T.P., Wilson, K.B., 1998, The estimation of energy and mass fluxes from vegetated surfaces. In: Proceedings of the 23rd Conference on Agricultural and Forest Meteorology, American Meteorolgical Society, Boston, MA, Preprints, pp. 163–166.

Pryor, S.C., Barthelmie, R., Carreiro, M.M., 1998. Measurement and modeling of carbon and nitrogen dynamics in a mid-latitude deciduous forest. Proposal submitted to National Institute for Global Environmental Change, US Department of Energy.

Randolph, J.C., 1998. Comparative analysis of carbon dynamics in a temperate deciduous forest in the mid-western United States. Proposal submitted to National Institute for Global Environmental Change, US Department of Energy.

Raupach, M.R., Coppin, P.A., Legg, B.J., 1986. Experiments on scalar dispersion within a plant canopy. Part I: The turbulence structure. Boundary-Layer Meteorol. 35, 21–52.

Raupach, M.R., Finnigan, J.J., Brunet, Y., 1996. Coherent eddies and turbulence in vegetation canopies. Boundary-Layer Meteorol. 78, 351–382.

Schimel, D.S., 1995. Terrestrial ecosystems and the carbon cycle. Global Change Biol. 1, 77–91.

Schmid, H.P., 1997. Experimental design for flux measurements: matching scales of observations and fluxes. Agric. For. Meteorol. 87, 179–200.

Shaw, R.H., Tavangar, J., 1983. Structure of the Reynolds stress in a canopy layer. J. Climate Appl. Meteorol. 22, 1922–1931.

Su, H.-B., Shaw, R.H., Paw U, K.T., Moeng, C.-H., Sullivan, P.P., 1998. Turbulent statistics of neutrally stratified flow within and above a Sparse Forest from large-eddy-simulation and field observations. Boundary-Layer Meteorol. 88, 363–397.

Su, H.B., Shaw, R.H., Paw U, K.T., 2000. Two-point correlation analysis of flow within and above a forest from large-eddy-simulation. Boundary-Layer Meteorol. 94, 423–460.

Tans, P.P., Fung, I.Y., Takahashi, T., 1990. Observational constraints on the global CO_2 budget. Science 247, 1431–1438.

Valentini, R., de Angelis, P., Matteucci, G., Monaco, R., Dore, S., Scarascia Mugnozza, G.E., 1996. Seasonal net carbon dioxide exchange of a beech forest with the atmosphere. Global Change Biol. 2, 199–207.

Vickers, D., Mahrt, L., 1997. Quality control and flux sampling problems for tower and aircraft data. J. Atmos. Ocean. Tech. 14, 512–526.

Von Kley, J.E., Parker, G.R., Franzmeier, D.P., Randolph, J.C., 1994. Field guide: ecological classification of the Hoosier National Forest and surrounding areas of Indiana. USDA Forest Service, 89 pp.

Webb, E.K., Pearman, G.J., Leuning, R., 1980. Correction of flux measurements for density effects due to heat and water vapor transfer. Quart. J. R. Meteorol. Soc. 106, 85–100.

Wofsy, S.C., Hollinger, D., 1997. Science plan for AmeriFlux: US long term flux measurement network. http://www.esd.ornl.gov/programs/NIGEC/sciplan2.html.

Wofsy, S.C., Goulden, M.L., Munger, J.W., Fan, S.-M., Bakwin, P.S., Daube, B.C., Bassow, S.L., Bazzaz, F.A., 1993. Net exchange of CO_2 in a mid-latitude forest. Science 260, 1314–1317.

Zhang, C., Shaw, R.H., Paw U, K.T., 1992. Spatial characteristics of turbulence coherent structures within and above an orchard canopy. In: Schwartz, S.E., Slinn, W.G.N. (Eds.), Precipitation Scavenging and Atmosphere-Surface Exchange. Hemisphere Publishing Co., Washington, pp. 741–751.